Three-baryon interaction generated by determinant interaction of quarks

AUTHOR(S):

Ohnishi, Akira; Kashiwa, Kouji; Morita, Kenji

PTEP

Prog. Theor. Exp. Phys. **2017**, 073D04 (19 pages)
DOI: 10.1093/ptep/ptx095

Three-baryon interaction generated by determinant interaction of quarks

Akira Ohnishi*, Kouji Kashiwa*, and Kenji Morita*

Yukawa Institute for Theoretical Physics, Kyoto University, Kyoto 606-8502, Japan
*E-mail: ohnishi@yukawa.kyoto-u.ac.jp; kouji.kashiwa@yukawa.kyoto-u.ac.jp; kmorita@yukawa.kyoto-u.ac.jp

Received January 8, 2017; Revised May 20, 2017; Accepted May 21, 2017; Published July 28, 2017

We discuss the 3-baryon interaction generated by the determinant interaction of quarks, known as the Kobayashi–Maskawa–'t Hooft (KMT) interaction. The expectation value of the KMT interaction operator is calculated in fully antisymmetrized quark-cluster model wave functions for 1-, 2-, and 3-octet-baryon states. The 3-baryon potential from the KMT interaction is found to be repulsive for $NN\Lambda$ and $N\Lambda\Lambda$ systems, while it is zero for the NNN system. The strength and range of the 3-baryon potential are found to be comparable to those for the NNN 3-body potential obtained in lattice QCD simulations. The contribution to the Λ single particle potential in nuclear matter is found to be 0.28 MeV and 0.73 MeV in neutron matter and symmetric nuclear matter at normal nuclear density, respectively. These repulsive forces are not enough to solve the hyperon puzzle, but may be measured in high-precision hyperisotope experiments.

Subject Index D00, D30, D41

1. Introduction

The discovery of 2-solar-mass neutron stars [1,2] has cast doubt on the equation of state (EOS) based on conventional nuclear physics. EOSs with nucleons and leptons for neutron star matter can support neutron stars whose masses are $M \sim 2M_\odot$, where $M_\odot$ is the solar mass. With hyperons (Y), however, the EOS generally becomes much softer and many of proposed EOSs cannot support $2M_\odot$ neutron stars [3–7]. This problem, referred to as the *hyperon puzzle*, has been attracting much attention.

Several mechanisms have been proposed so far to solve the hyperon puzzle. One of the ideas is to assume that the crossover transition [8,9] from nuclear matter to quark matter takes place at relatively low density, 2–3ρ_0, with $\rho_0 \simeq 0.16\,\mathrm{fm}^{-3}$ being the normal nuclear matter density, instead of the often assumed first-order deconfinement phase transition at high density. In this case, the transition may occur at lower density than the onset of hyperon mixing via the weak interaction, and then prevents the matter from softening owing to the emergence of the hyperons. The crossover nature of the transition also circumvents the softening from the first-order phase transition. This crossover picture can be examined by making use of high-energy heavy-ion collision experiments. Indeed, the direct flow collapse in Au+Au collisions at $\sqrt{s_{NN}} = 11.5$ GeV [10] seems to suggest the sudden softening of EOS [11], which could be caused by the first-order phase transition. Further studies including the isospin asymmetry dependence of the phase transition order are necessary to examine the crossover transition in dense neutron-rich matter. Another idea is to modify the

hyperon–nucleon (YN) interaction. Within the flavor SU(3) coupling scheme but off the flavor-spin SU(6) couplings, one can obtain a stiff hyperonic matter EOS [12] with parameters including large $\bar{s}s$ contents in nucleons, which, however, contradicts the recent lattice QCD calculations; see Ref. [13] and references therein. The third idea is to introduce the 3-baryon ($3B$) interaction involving hyperons If the 3-nucleon ($3N$) force is repulsive and there exist repulsive $3B$ forces involving hyperons, the EOS can support $2M_\odot$ neutron stars by suppressing hyperon mixing at high densities.

The role of the $3N$ force has been extensively discussed in nuclear physics. Ab initio calculations with 2-nucleon interactions cannot reproduce the binding energies of 3-nucleon systems (t and ^{3}He) and the nuclear matter saturation point, and it has been noticed that a 3-nucleon ($3N$) force is necessary to reproduce these fundamental aspects of nucleon many-body systems [14–21]. The $3N$ force contains a 2-pion P-wave exchange term with an intermediate Δ excitation (Fujita–Miyazawa force) [14] and a shorter-range phenomenological term [15]. One of the physical pictures of the short-range $3N$ force is the multi-pomeron exchange [16]. Recently, the $3N$ force has been derived systematically in the chiral effective field theory, where energy-independent $3N$ forces appear at the next-to-next-to-leading order [17,18]. Microscopic calculations including these $3N$ forces show that the $3N$ force is relevant to the nuclear matter saturation and the nuclear matter EOS at high densities [15,16,19–21], and also to deuteron–proton scattering observables [22]. Moreover, there has been remarkable progress in the lattice QCD simulation for the $3N$ force based on the Nambu–Bethe–Salpeter wave function, i.e., the HAL QCD method [23]. At present, such lattice QCD simulations have been performed for larger π masses than the physical π mass and then their data still have large error bars. Cooperations between lattice QCD simulations, experiments, and phenomenological approaches including the present study should play an important role in understanding the nature of the $3N$ force and also other $3B$ forces in future.

So far $3B$ forces involving hyperons have not been known well. Since the currently available hypernuclear data are not enough to determine the $3B$ force involving hyperons precisely at the level of the $3N$ force, then we have to rely on some models or assumptions. In Ref. [16], the repulsive $3B$ forces are assumed to work universally for YNN, YYN, YYY as well as for NNN in the multi-pomeron exchange mechanism. By fixing the multi-pomeron exchange strength by the nuclear elastic scattering, the nuclear matter saturation and hypernuclear separation energies are reproduced in the G-matrix calculations, and $2M_\odot$ neutron stars are found to be supported. In Ref. [24], the authors adopt a phenomenological hyperon–nucleon potential, which contains ΛN forces consistent with the Λp scattering data and a strongly repulsive Wigner-type ΛNN force [25]. The Λ separation energies are well reproduced in the auxiliary field diffusion Monte Carlo calculations, and the EOS fitted to the Monte Carlo results can support $2M_\odot$ neutron stars when the ΛNN forces are included [26]. In this treatment, the Λ separation energies in heavy Λ hypernuclei are calculated to be more than 60 MeV with the 2-body ($2B$) forces, while they are reduced to be less than 30 MeV with the $3B$ forces. The effects of the $3B$ potential are very large, and it is natural to deduce that the 4- and more baryon potential would be as important as the $3B$ potential. In Ref. [27], internal structure modification of baryons is taken into account in the framework of the chiral quark meson coupling model. The modification leads to the σ dependence of the baryon–σ coupling, or the baryon–σ–σ multi-body coupling, where σ is the isoscalar scalar meson field. Because of the multi-body coupling and the Fock term contribution, hyperons are suppressed at high densities, and $2M_\odot$ neutron stars can be supported within the observation errors. While these approaches are successful in explaining the existence of $2M_\odot$ neutron stars with EOS including hyperons, it is preferable to derive the $3B$ interaction from the viewpoint of the quark dynamics.

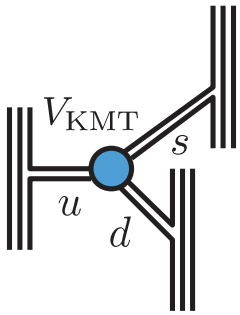

Fig. 1. Schematic picture of 3-baryon interaction generated by the KMT interaction.

One of the possible origins of the $3B$ interaction is the determinant interaction of quarks, referred to as the Kobayashi–Maskawa–'t Hooft (KMT) interaction [28–31],

$$\mathcal{L}_{\rm KMT} = g_{\rm D}\ (\det\Phi + \text{h.c.}), \tag{1}$$

$$\Phi_{ij} = \bar{q}_j(1-\gamma_5)q_i, \tag{2}$$

where det denotes the determinant with respect to the flavor indices i and j. With 3 flavors of quarks ($N_f = 3$), the KMT interaction replaces 3 quarks having different flavors with 3 quarks, then it can generate the $3B$ interaction; The $3B$ system having at least one u, d, and s quark can be connected by the KMT interaction as shown schematically in Fig. 1.

The KMT interaction was introduced in order to account for the axial U(1) (U(1)$_A$) anomaly [28,29], and it was found to be generated by instantons [30,31]. The strength of the KMT interaction $g_{\rm D}$ can be fixed by reproducing basic quantities of mesons. For example, $g_{\rm D}$ was determined to be $g_{\rm D}\Lambda^5 = -9.29$ [32] or $g_{\rm D}\Lambda^5 = -12.36$ [33] in the Nambu–Jona-Lasinio (NJL) model [34,35] by fitting the π, K, and η' masses and the pion decay constant with other model parameters. Since the U(1)$_A$ anomaly pushes up the η' mass ($m_{\eta'}$), the value of $g_{\rm D}$ is essentially fixed by $m_{\eta'}$ [32]. By comparison, the $g_{\rm D}$ value fitted to the $\eta \to \gamma\gamma$ decay width is found to be about 4 times larger than that from fitting to the η' mass [36], and the strength of the instanton-induced interaction may be much stronger in the instanton liquid picture of the QCD vacuum [37]. This difference may come from the lack of the confinement mechanism in the NJL model [36]. Thus the strength of the KMT interaction has uncertainty, and the 3-baryon potential shown later may be enhanced by some factor.

From the above considerations, the $3B$ interaction from the KMT interaction has favorable features to resolve the hyperon puzzle. It acts only on systems including strange quarks, and it is probably repulsive because of the negative value of $g_{\rm D}$. In the mean-field treatment for the NJL model, the KMT interaction pushes up the constituent quark mass [32], $M_u = m_u - 2g_s\langle\bar{u}u\rangle - 2g_{\rm D}\langle\bar{d}d\rangle\langle\bar{s}s\rangle$, $M_d = m_d - 2g_s\langle\bar{d}d\rangle - 2g_{\rm D}\langle\bar{s}s\rangle\langle\bar{u}u\rangle$, and $M_s = m_s - 2g_s\langle\bar{s}s\rangle - 2g_{\rm D}\langle\bar{u}u\rangle\langle\bar{d}d\rangle$, where $m_{u,d,s}$ represent the current quark mass, g_s is the 4-fermion scalar coupling, and $\langle\bar{q}q\rangle < 0$ is the quark condensate. The KMT interaction is found to act repulsively also in the $\Lambda\Lambda$ interaction [38]. While the color-magnetic interaction is strongly attractive in the flavor singlet 6-quark state, the H dibaryon [39], the KMT interaction acts repulsively and the mass of H may be pushed up above the $\Lambda\Lambda$ threshold.

In this article, we discuss the $3B$ interaction generated by the KMT interaction in the quark-cluster model. We adopt here the nonrelativistic treatment for the wave functions of quarks and the KMT interaction. We consider the nonrelativistic wave functions of quarks in baryons, and the spatial wave

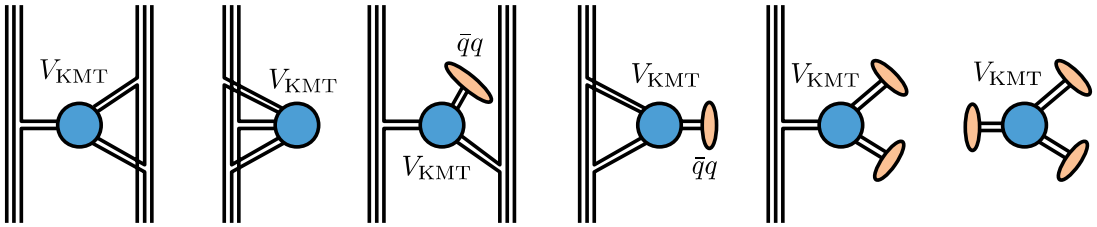

Fig. 2. Other interaction terms from the KMT interaction.

function is assumed to be $(0s)^3$; all quarks are assumed to be in the s-wave state of the harmonic oscillator potential and to have the same spatial extension. In the nonrelativistic treatment of the KMT interaction, we ignore the γ_5 part in Φ_{ij}, then the KMT interaction becomes the zero-range 3-body interaction among quarks (6-fermi interaction), which modifies the flavor but does not modify the spin and color of quarks. It should be noted that the present treatment of the 3-quark potential from the KMT interaction is different from the instanton-induced interaction obtained in Ref. [40], where the lower components of quarks are also considered. Furthermore, we here concentrate on the 3-quark potential part from the KMT interaction, the diagram in Fig. 1 and the first two diagrams in Fig. 2, since only the 3-quark potential part generates 3-baryon interaction. In this treatment, we do not need to set the quark condensate $\langle\bar{q}q\rangle$, which appears in other diagrams in Fig. 2, and there is no contribution to the $N-\Delta$ mass difference [37], since we need u, d, and s quarks in the 3 quarks for the KMT interaction to work.

This paper is organized as follows. In Sect. 2, we evaluate the norms of the 1-, 2-, and 3-baryon wave functions in the quark-cluster model. In Sect. 3, we quantify the $3B$ potential generated by the KMT interaction based on the 3-baryon wave function and discuss its implication to the hyperon puzzle. Section 4 is devoted to a summary.

2. Quark-cluster model wave function

2.1. *One-baryon state*

We consider here the flavor-spin SU(6) wave function of octet baryons. For example, the color, flavor, spin wave function for $n_\uparrow$, $n_\downarrow$, and $\Lambda_\uparrow$ are given as

$$\psi(n_\uparrow) = \frac{1}{\sqrt{3!}}\frac{1}{2\sqrt{3}}\varepsilon_{abc}\left[d_\uparrow d_\downarrow u_\uparrow + d_\downarrow d_\uparrow u_\uparrow - 2d_\uparrow d_\uparrow u_\downarrow\right]^{abc}, \tag{3}$$

$$\psi(n_\downarrow) = \frac{1}{\sqrt{3!}}\frac{1}{2\sqrt{3}}\varepsilon_{abc}\left[d_\downarrow d_\uparrow u_\downarrow + d_\uparrow d_\downarrow u_\downarrow - 2d_\downarrow d_\downarrow u_\uparrow\right]^{abc}, \tag{4}$$

$$\psi(\Lambda_\uparrow) = \frac{1}{\sqrt{3!}}\frac{1}{\sqrt{2}}\varepsilon_{abc}\left[u_\uparrow d_\downarrow s_\uparrow - u_\downarrow d_\uparrow s_\uparrow\right]^{abc}, \tag{5}$$

where ε_{abc} is the Levi-Civita tensor with respect to color indices. The first $1/\sqrt{3!}$ factor is the color symmetry factor, which is common to all baryons. The normalization factor is determined to normalize the fully antisymmetrized wave function, $\psi_{\mathcal{A}} = \mathcal{A}/\sqrt{3!}\times\psi$. The antisymmetrizer $\mathcal{A}$ is defined as

$$\mathcal{A}[q_1 q_2\cdots q_n] = \sum_P \mathrm{sgn}(P)\, q_{P(1)}q_{P(2)}\cdots q_{P(n)}, \tag{6}$$

Table 1. Octet baryon wave functions with the spin-up state. The fully antisymmetrized wave function is given as $|\psi_{\mathcal{A}}\rangle = \mathcal{A}/\sqrt{3!} \times \varepsilon_{abc}/\sqrt{3!} \times [|\text{Flavor}\rangle \otimes |\text{Spin}\rangle \otimes |\text{Spatial w.f.}\rangle]^{abc}$.

B	$\|\text{Flavor}\rangle$	$\|\text{Spin}\rangle$
$n_\uparrow$	$\|ddu\rangle/\sqrt{2}$	$\|\uparrow\downarrow\uparrow + \downarrow\uparrow\uparrow - 2\uparrow\uparrow\downarrow\rangle/\sqrt{6}$
$p_\uparrow$	$\|uud\rangle/\sqrt{2}$	$\|\uparrow\downarrow\uparrow + \downarrow\uparrow\uparrow - 2\uparrow\uparrow\downarrow\rangle/\sqrt{6}$
$\Lambda_\uparrow$	$\|uds\rangle$	$\|\uparrow\downarrow\uparrow - \downarrow\uparrow\uparrow\rangle/\sqrt{2}$
$\Sigma^-_\uparrow$	$\|dds\rangle/\sqrt{2}$	$\|\uparrow\downarrow\uparrow + \downarrow\uparrow\uparrow - 2\uparrow\uparrow\downarrow\rangle/\sqrt{6}$
$\Sigma^0_\uparrow$	$\|uds\rangle$	$\|\uparrow\downarrow\uparrow + \downarrow\uparrow\uparrow - 2\uparrow\uparrow\downarrow\rangle/\sqrt{6}$
$\Sigma^+_\uparrow$	$\|uus\rangle/\sqrt{2}$	$\|\uparrow\downarrow\uparrow + \downarrow\uparrow\uparrow - 2\uparrow\uparrow\downarrow\rangle/\sqrt{6}$
$\Xi^-_\uparrow$	$\|ssd\rangle/\sqrt{2}$	$\|\uparrow\downarrow\uparrow + \downarrow\uparrow\uparrow - 2\uparrow\uparrow\downarrow\rangle/\sqrt{6}$
$\Xi^0_\uparrow$	$\|ssu\rangle/\sqrt{2}$	$\|\uparrow\downarrow\uparrow + \downarrow\uparrow\uparrow - 2\uparrow\uparrow\downarrow\rangle/\sqrt{6}$

where P denotes permutation, q_i is the quark wave function, and $\text{sgn}(P)$ is the sign (or signature) of the permutation P. The flavor and spin wave functions for octet baryons are summarized in Table 1 for completeness.

The norm of the 1-baryon state is obtained as

$$\begin{aligned}\mathcal{N}_{\mathcal{A}} &\equiv \langle\psi_{\mathcal{A}}(n_\uparrow) \mid \psi_{\mathcal{A}}(n_\uparrow)\rangle = \frac{1}{3!}\langle\mathcal{A}[\psi(n_\uparrow)] \mid \mathcal{A}[\psi(n_\uparrow)]\rangle = \langle\psi(n_\uparrow) \mid \mathcal{A}[\psi(n_\uparrow)]\rangle \\ &= \frac{1}{3!}\sum_{i,j} c_i^* c_j \langle\varepsilon_{abc}\phi_i^{abc}(n_\uparrow) \mid \mathcal{A}[\varepsilon_{def}\phi_j^{def}(n_\uparrow)]\rangle \\ &= \sum_{i,j} c_i^* c_j \langle\phi_i(n_\uparrow) \mid [\mathcal{S}_{\text{fss}}\,\phi_j(n_\uparrow)]\rangle_{\text{fss}} = \sum_{i,j} c_i^* c_j \sum_P F_P(\phi_i,\phi_j),\end{aligned} \tag{7}$$

where $c_i = 1/2\sqrt{3}, 1/2\sqrt{3}, -1/\sqrt{3}$ $(i = 1,2,3)$ and $\phi_i = d_\uparrow d_\downarrow u_\uparrow, d_\downarrow d_\uparrow u_\uparrow, d_\uparrow d_\uparrow u_\downarrow$ $(i = 1,2,3)$ are the flavor-spin coefficient and component of the 1-baryon wave function, respectively. The antisymmetrizer $\mathcal{A}$ acts on the color, flavor, spin, and spatial coordinate wave functions, while the symmetrizer in the flavor-spin-spatial (fss) coordinates $\mathcal{S}_{\text{fss}}$ does not exchange color indices. In the last line, the matrix element is obtained in the flavor, spin, and spatial coordinate wave functions $F_P(\phi_i,\phi_j) = \langle\phi_i \mid P\phi_j\rangle_{\text{fss}}$. For example, one of the elements looks like

$$\begin{aligned}\langle\phi_1(n_\uparrow) \mid [\mathcal{S}_{\text{fss}}\,\phi_2(n_\uparrow)]\rangle_{\text{fss}} &= \sum_P F_P(\phi_1,\phi_2) \\ &= \langle d_\uparrow d_\downarrow u_\uparrow \mid d_\downarrow d_\uparrow u_\uparrow + d_\uparrow u_\uparrow d_\downarrow + u_\uparrow d_\downarrow d_\uparrow + d_\downarrow u_\uparrow d_\uparrow + u_\uparrow d_\uparrow d_\downarrow + d_\uparrow d_\downarrow u_\uparrow\rangle_{\text{fss}} = 1,\end{aligned} \tag{8}$$

provided that the spatial wave function is common to all quarks and normalized.

2.2. *Two-baryon states*

Two-baryon states are defined as the product of 2-baryon wave functions fully antisymmetrized in color, flavor, spin, and spatial coordinates. As an example, we show the case of $n_\uparrow n_\downarrow$,

$$|\psi_{\mathcal{A}}(n_\uparrow, n_\downarrow)\rangle = \frac{1}{\sqrt{6!}}|\mathcal{A}[\psi(n_\uparrow)\psi(n_\downarrow)]\rangle. \tag{9}$$

The norm of the above 2-baryon state is obtained as

$$\begin{aligned}\mathcal{N}_{\mathcal{A}} &= \langle \psi_{\mathcal{A}}(n_\uparrow, n_\downarrow) \mid \psi_{\mathcal{A}}(n_\uparrow, n_\downarrow)\rangle \\ &= \langle \psi(n_\uparrow)\psi(n_\downarrow) \mid \mathcal{A}[\psi(n_\uparrow)\psi(n_\downarrow)]\rangle \\ &= \frac{1}{(3!)^2}\sum_{i,j,k,l} c_i^*(n_\uparrow)c_j^*(n_\downarrow)c_k(n_\uparrow)c_l(n_\downarrow)\,\varepsilon_{abc}\,\varepsilon_{def}\,\varepsilon_{a'b'c'}\,\varepsilon_{d'e'f'} \\ &\quad\times \langle \phi_i^{abc}(n_\uparrow)\phi_j^{def}(n_\downarrow) \mid \mathcal{A}\,[\phi_k^{a'b'c'}(n_\uparrow)\phi_l^{d'e'f'}(n_\downarrow)]\rangle \\ &= \sum_{i,j,k,l} c_i^*(n_\uparrow)c_j^*(n_\downarrow)c_k(n_\uparrow)c_l(n_\downarrow)\sum_P C_P(\phi_i\phi_j,\phi_k\phi_l)\,F_P(\phi_i\phi_j,\phi_k\phi_l). \end{aligned} \tag{10}$$

The color and flavor–spin–spatial factors are shown by C_P and F_P. The exchange of quarks among baryons gives rise to a sign factor, which cannot be absorbed in the Levi-Civita tensor ε,

$$\mathcal{A}[1^a1^b1^c2^d2^e2^f] = 1^a1^b1^c2^d2^e2^f - 1^a1^b2^d1^c2^e2^f + 1^a2^e2^d1^c1^b2^f + \cdots, \tag{11}$$

where 1^a (2^d) shows one of the quarks in the first (second) baryon having the color index a (d). The color factor is obtained as the contraction of ε. For the case of the second term in Eq. (11), the first (second) three colors in the bra state need to be abd (cef) to have a finite matrix element, and we obtain

$$C_P = -\frac{1}{(3!)^2}\varepsilon_{abd}\varepsilon_{cef}\varepsilon_{abc}\varepsilon_{def} = -\frac{1}{36}\,2\delta_{dc}\,2\delta_{cd} = -\frac{1}{3}. \tag{12}$$

The color factor in the 2-baryon case is found to be $C_P = 1, -1/3, 1/3, -1$ for 0-, 1-, 2- and 3-quark exchanges between baryons, respectively. The flavor–spin–spatial factor for the permutation P is

$$F_P(\phi_i\phi_j,\phi_k\phi_l) = \langle \phi_i(n_\uparrow)\phi_j(n_\downarrow) \mid P[\phi_k(n_\uparrow)\phi_l(n_\downarrow)]\rangle_{\rm fss} = 0 \text{ or } 1, \tag{13}$$

provided that 2 baryons are located at the same spatial point.

2.3. *Three-baryon states*

Three-baryon states are defined in a way similar to the 2-baryon states. For the $n_\uparrow n_\downarrow \Lambda_\uparrow$ state, the 3-baryon wave function reads

$$|\psi_{\mathcal{A}}(n_\uparrow, n_\downarrow, \Lambda_\uparrow)\rangle = \frac{1}{\sqrt{9!}}|\mathcal{A}[\psi(n_\uparrow)\psi(n_\downarrow)\psi(\Lambda_\uparrow)]\rangle. \tag{14}$$

The norm of the 3-baryon state is obtained as

$$\begin{aligned}\mathcal{N}_{\mathcal{A}} &= \langle \psi_{\mathcal{A}}(n_\uparrow, n_\downarrow, \Lambda_\uparrow) \mid \psi_{\mathcal{A}}(n_\uparrow, n_\downarrow, \Lambda_\uparrow)\rangle \\ &= \langle \psi(n_\uparrow)\psi(n_\downarrow)\psi(\Lambda_\uparrow) \mid \mathcal{A}[\psi(n_\uparrow)\psi(n_\downarrow)\psi(\Lambda_\uparrow)]\rangle \\ &= \frac{1}{(3!)^3}\sum_{i,j,k,l,m,n} c_{ijk}^*(n_\uparrow n_\downarrow \Lambda_\uparrow)c_{lmn}(n_\uparrow n_\downarrow \Lambda_\uparrow)\,\varepsilon_{abc}\,\varepsilon_{def}\,\varepsilon_{ghi}\,\varepsilon_{a'b'c'}\,\varepsilon_{d'e'f'}\,\varepsilon_{g'h'i'} \\ &\quad\times \langle \phi_i^{abc}(n_\uparrow)\phi_j^{def}(n_\downarrow)\phi_k^{ghi}(\Lambda_\uparrow) \mid \mathcal{A}\,[\phi_l^{a'b'c'}(n_\uparrow)\phi_m^{d'e'f'}(n_\downarrow)\phi_n^{g'h'i'}(\Lambda_\uparrow)]\rangle \\ &= \sum_{i,j,k,l,m,n} c_{ijk}^*(n_\uparrow n_\downarrow \Lambda_\uparrow)c_{lmn}(n_\uparrow n_\downarrow \Lambda_\uparrow)\sum_P C_P(\phi_{ijk},\phi_{lmn})\,F_P(\phi_{ijk},\phi_{lmn}), \end{aligned} \tag{15}$$

where $c_{ijk}(B_1B_2B_3) = c_i(B_1)c_j(B_2)c_k(B_3)$, $\phi_{ijk} = \phi_i\phi_j\phi_k$, and C_P and F_P are the color and flavor–spin–spatial factors, respectively.

Calculation of the color factor for the 3-baryon states is straightforward but lengthy. We show one of the nontrivial examples:

$$\begin{aligned} &-\frac{1}{(3!)^3}\varepsilon_{abc}\varepsilon_{def}\varepsilon_{ghi}\varepsilon_{a'b'c'}\varepsilon_{d'e'f'}\varepsilon_{g'h'i'}\langle 1^a1^b1^c2^d2^e2^f3^g3^h3^i \mid 1^{a'}1^{b'}3^{g'}2^{d'}3^{h'}3^{i'}1^{c'}2^{e'}2^{f'}\rangle \\ &\quad = -\frac{1}{(3!)^3}\varepsilon_{abc}\varepsilon_{def}\varepsilon_{ghi}\varepsilon_{abg}\varepsilon_{dhi}\varepsilon_{cef}\langle 111222333 \mid 113233122\rangle_{\rm fss} \\ &\quad = -\frac{1}{9}\langle 111222333 \mid 113233122\rangle_{\rm fss}. \end{aligned} \tag{16}$$

In this case the color factor is $C_P = -1/9$.

Exchanges of quarks among 3 baryons can be categorized into the following types:

(a1) Direct term (no quark exchange) (D).
(a2) Cyclic baryon exchange (BC).
(a3) Baryon exchange (BX).
(b1) 1-quark-pair exchange between 2 baryons (1QX).
(b2) 1-quark-pair exchange between 2 baryons after cyclic baryon exchange (1QX+BC).
(b3) 1-quark-pair exchange between 2 baryons after baryon exchange of the different baryon pair (1QX+BX).
(b4) 1-quark-pair exchange between 2 baryons after baryon exchange of the same baryon pair (1QX+BXs) (or 2-quark pair exchange between 2 baryons).
(c1) 2-quark-pair exchange among 3 baryons with a stand baryon (2QX).
(c2) 2-quark-pair exchange among 3 baryons with a stand baryon after cyclic baryon exchange (2QX+BC).
(c3) 2-quark-pair exchange among 3 baryons with a stand baryon after baryon exchange (2QX+BX).
(d1) Cyclic 3-quark exchange (QC).
(d2) Cyclic 3-quark exchange after cyclic baryon exchange (QC+BC).
(d3) Cyclic 3-quark exchange after baryon exchange (QC+BX).
(e) Cyclic 3-quark and anti-cyclic 3-quark exchange among 3 baryons (QC+QA).

We schematically show the corresponding diagrams for these types in Fig. 3.

We find that the color factor is ± 1 when there is no quark exchange among baryons (a1, a2, a3). When 1 baryon keeps its 3 quarks (b1–b4), the color factor is $\pm 1/3$. In the case where all 3 baryons are involved in quark exchanges, the color factor is $\pm 1/9$ in most of the cases (c1–c3, d1–d3). The single exception is (e), $C_P = 0$, where the ket state is made of 3 baryons, each of which contains 1 quark from each baryon in the bra state. We summarize the color factor in Table 2, and the norm in some of 2- and 3-baryon systems in Table 3.

The norm of the 3-baryon states can be more elegantly evaluated by using the reduction formula of the antisymmetrizer for the 3 octet baryon states [41,42],

$$\begin{aligned} \mathcal{A} &= [1 - 9(P_{36} + P_{39} + P_{69}) + 27(P_{369} + P_{396}) + 54(P_{25}P_{39} + P_{35}P_{69} + P_{38}P_{69})]\,\mathcal{A}_B \\ &\quad - 216P_{25}P_{38}P_{69}, \end{aligned} \tag{17}$$

$$\mathcal{A}_B = \sum_{\mathcal{P}}(-1)^{\pi(\mathcal{P})}\mathcal{P}, \tag{18}$$

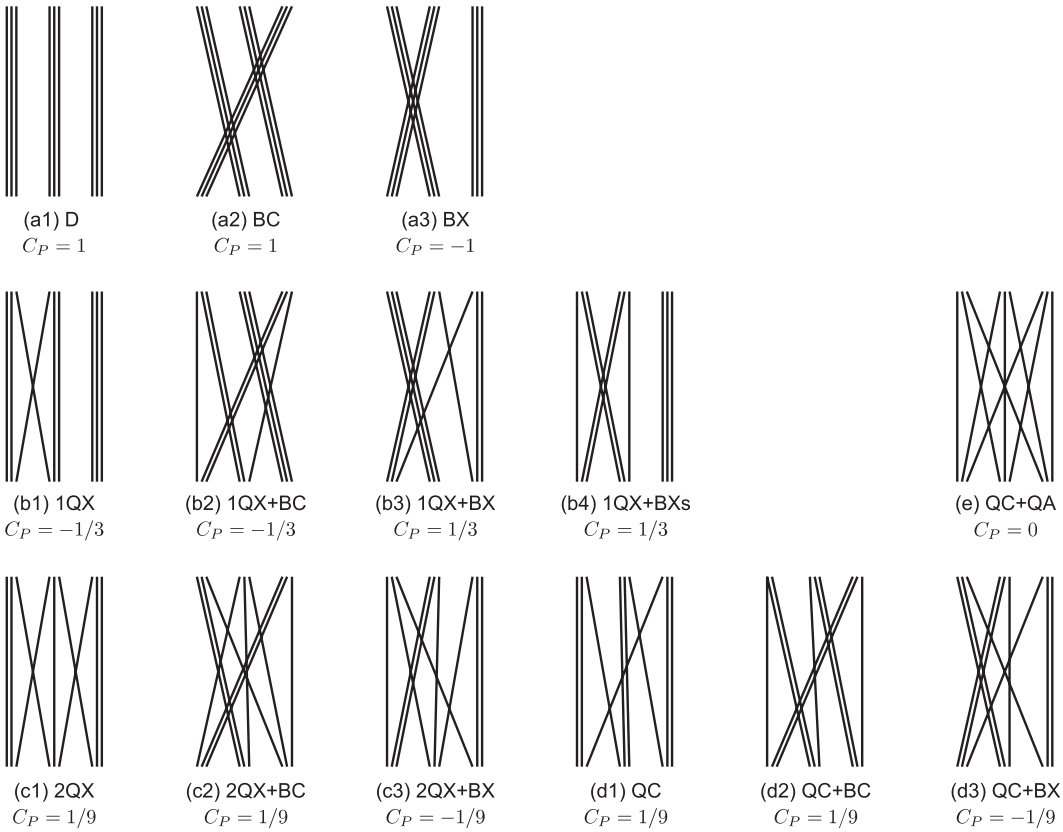

Fig. 3. Quark exchange diagrams and the corresponding color factor. See the text for the description of the quark exchanges.

where P_{ij} denotes the exchange operator of the ith and jth quarks, P_{ijk} denotes the cyclic exchange operator of the ijkth quarks, and $\mathcal{P}$ is the baryon exchange operator with $\pi(\mathcal{P})$ being its signature. Equation (17) takes care of 1680 permutations, which act on $(3!)^3 = 216$ terms in the product of 3 antisymmetrized baryon wave functions and result in $1680 \times 216 = 9!$ permutations. In our categorization, the first, second, third, and fourth terms in the first line of Eq. (17) correspond to (a1–a3), (b1–b4), (d1–d3), and (c1–c3), respectively, and the second line corresponds to type (e).

3. Expectation value of the KMT operator and 3-baryon potential

3.1. KMT operator and its expectation value

We now evaluate the KMT matrix elements in 1-, 2-, and 3-baryon systems. We concentrate on the $(0s)^6$ and $(0s)^9$ configurations of quarks for 2- and 3-baryon systems, respectively, which correspond to the cases where 2 or 3 baryons are located at the same spatial point.

In the nonrelativistic treatment of the KMT interaction (2), we ignore terms that involve γ_5 and replace γ_0 with a unit matrix in Φ_{ij},

$$V_{\rm KMT} \simeq -2g_{\rm D} \int d^3x\, \varepsilon_{ijk}\, u^\dagger(\boldsymbol{x}) q_i(\boldsymbol{x})\, d^\dagger(\boldsymbol{x}) q_j(\boldsymbol{x})\, s^\dagger(\boldsymbol{x}) q_k(\boldsymbol{x})\,. \tag{19}$$

Table 2. Color factor. See the text for the quark exchange.

Permutation	C_P	Type
111 222 333	1	D (a1)
222 333 111	1	BC (a2)
333 111 222	1	
111 333 222	−1	BX (a3)
333 222 111	−1	
222 111 333	−1	
111 223 233	−1/3	1QX (b1)
113 222 133	−1/3	
112 122 333	−1/3	
133 113 222	−1/3	1QX+BC (b2)
333 112 122	−1/3	
233 111 223	−1/3	
223 233 111	−1/3	
222 133 113	−1/3	
122 333 112	−1/3	
113 133 222	1/3	1QX+BX (b3)
112 333 122	1/3	
233 223 111	1/3	
333 122 112	1/3	
223 111 233	1/3	
222 113 133	1/3	
111 233 223	1/3	1QX+BXs(b4)
133 222 113	1/3	
122 112 333	1/3	
123 122 133	1/9	2QX (c1)
112 123 233	1/9	
113 223 123	1/9	
123 113 223	1/9	2QX+BC (c2)
133 123 122	1/9	
233 112 123	1/9	
123 233 112	1/9	
223 123 113	1/9	
122 133 123	1/9	
113 123 223	−1/9	2QX+BX (c3)
112 233 123	−1/9	
123 133 122	−1/9	
123 223 113	−1/9	
233 123 112	−1/9	
133 122 123	−1/9	
123 112 233	−1/9	
122 123 133	−1/9	
223 113 123	−1/9	
112 223 133	1/9	QC (d1)
113 122 233	1/9	
233 113 122	1/9	QC+BC (d2)
133 112 223	1/9	
122 233 113	1/9	
223 133 112	1/9	
112 133 223	−1/9	QC+BX (d3)
113 233 122	−1/9	
133 223 112	−1/9	
233 122 113	−1/9	
223 112 133	−1/9	
122 113 233	−1/9	
123 123 123	0	QC+QA (e)

Then we obtain the matrix element of the KMT interaction for the 3-quark states having a common color configuration as

$$\begin{aligned}
&\langle q_1 q_2 q_3 \mid V_{\rm KMT} \mid q'_1 q'_2 q'_3 \rangle \\
&\quad = -2g_{\rm D} \sum_{\{\alpha,\beta,\gamma\}} \int d^3x\, \varepsilon_{ijk} \langle q_\alpha \mid u^\dagger(\boldsymbol{x}) q_i(\boldsymbol{x}) \mid q'_\alpha \rangle \langle q_\beta \mid d^\dagger(\boldsymbol{x}) q_j(\boldsymbol{x}) \mid q'_\beta \rangle \langle q_\gamma \mid s^\dagger(\boldsymbol{x}) q_k(\boldsymbol{x}) \mid q'_\gamma \rangle \\
&\quad = -2g_{\rm D}\, \varepsilon_{ijk} \sum_{\{\alpha,\beta,\gamma\}} \langle q_\alpha \mid \hat{T}^{u,i} \mid q'_\alpha \rangle_{\rm fs} \langle q_\beta \mid \hat{T}^{d,j} \mid q'_\beta \rangle_{\rm fs} \langle q_\gamma \mid \hat{T}^{s,k} \mid q'_\gamma \rangle_{\rm fs} \int d^3x \prod_\mu \varphi^*_\mu(\boldsymbol{x}) \varphi'_\mu(\boldsymbol{x}),
\end{aligned} \tag{20}$$

where the operator $\hat{T}^{i,j}$ replaces the flavor j with the flavor i, and $\varphi_\alpha(\boldsymbol{x})$ ($\varphi'_\alpha(\boldsymbol{x})$) shows the spatial part of the αth quark wave function in the bra (ket) state. We find the quantum mechanical KMT

Table 3. Norm and diagonal matrix elements of the KMT operator in 2- and 3-baryon systems of N and Λ. The $2B$ and $3B$ matrix elements are evaluated by subtracting the contribution of subsystems (see text). For the 1-baryon state, the norm is unity and the KMT diagonal matrix element is zero.

Baryon(s)	$\mathcal{N}_\mathcal{A}$	$\mathcal{T}_\mathcal{A}$	$\mathcal{T}$	$\mathcal{T}_{nB}$ $(n=2,3)$
$(NN)_{(S,T)=(0,1),(1,0)}$	10/9	0	0	0
$N_\uparrow\Lambda_\uparrow, N_\downarrow\Lambda_\downarrow$	1	20/3	20/3	20/3
$N_\uparrow\Lambda_\downarrow, N_\downarrow\Lambda_\uparrow$	1	10/3	10/3	10/3
$(\Lambda\Lambda)_{S=0}$	1	18/3	18/3	18/3
$(NNN)_{(S,T)=(1/2,1/2)}$	100/81	0	0	0
$n_\uparrow n_\downarrow\Lambda, p_\uparrow p_\downarrow\Lambda$	25/27	350/27	14	12/3
$n_\uparrow p_\uparrow\Lambda_\uparrow, n_\downarrow p_\downarrow\Lambda_\downarrow$	25/27	750/27	30	50/3
$n_\uparrow p_\uparrow\Lambda_\downarrow, n_\downarrow p_\downarrow\Lambda_\uparrow$	25/27	250/27	10	10/3
$n_\uparrow p_\downarrow\Lambda, n_\downarrow p_\uparrow\Lambda$	25/27	425/27	17	21/3
$N\Lambda_\uparrow\Lambda_\downarrow$	45/54	1035/54	23	21/3

interaction operator as,

$$V_{\rm KMT} = -2g_{\rm D}\varepsilon_{ijk}\sum_{\{\alpha,\beta,\gamma\}}\hat{T}^{u,i}_\alpha\,\hat{T}^{d,j}_\beta\,\hat{T}^{s,k}_\gamma\,\delta(\boldsymbol{x}_\alpha-\boldsymbol{x}_\beta)\delta(\boldsymbol{x}_\beta-\boldsymbol{x}_\gamma). \tag{21}$$

The operator $\hat{T}^{i,j}_\alpha$ now acts on the αth quark. For more generic product wave functions with the same color configurations, $\phi=\prod_\alpha q_\alpha$ and $\phi'=\prod_\alpha q'_\alpha$, the KMT matrix element is found to be

$$\begin{aligned}\langle\phi\mid V_{\rm KMT}\mid\phi'\rangle &= \sum_{\{\alpha,\beta,\gamma\}}\langle q_\alpha q_\beta q_\gamma\mid V_{\rm KMT}\mid q'_\alpha q'_\beta q'_\gamma\rangle\prod_{i\neq\{\alpha,\beta,\gamma\}}\langle q_i\mid q'_i\rangle\\ &= -2g_{\rm D}\,\langle\sigma\mid\sigma'\rangle\sum_{\{\alpha,\beta,\gamma\}}F^{\rm KMT}_{\alpha\beta\gamma}(f,f')R^{\rm KMT}_{\alpha\beta\gamma}(\varphi,\varphi'),\end{aligned} \tag{22}$$

$$\langle\sigma\mid\sigma'\rangle = \prod_\alpha\langle\sigma_\alpha\mid\sigma'_\alpha\rangle, \tag{23}$$

$$\begin{aligned}F^{\rm KMT}_{\alpha\beta\gamma}(f,f') &= \langle f\mid\varepsilon_{ijk}\,\hat{T}^{u,i}_\alpha\,\hat{T}^{d,j}_\beta\,\hat{T}^{s,k}_\gamma\mid f'\rangle\\ &= \delta_{u,f_\alpha}\delta_{d,f_\beta}\delta_{s,f_\gamma}\sum_{ijk}\varepsilon_{ijk}\,\delta_{i,f'_\alpha}\delta_{j,f'_\beta}\delta_{k,f'_\gamma}\prod_{\mu\neq\{\alpha,\beta\,\gamma\}}\delta_{f_\mu,f'_\mu},\end{aligned} \tag{24}$$

$$\begin{aligned}R^{\rm KMT}_{\alpha\beta\gamma}(\varphi,\varphi') &= \langle\varphi\mid\delta(\boldsymbol{x}_\alpha-\boldsymbol{x}_\beta)\delta(\boldsymbol{x}_\beta-\boldsymbol{x}_\gamma)\mid\varphi'\rangle\\ &= \int d^3x\varphi^*_\alpha(\boldsymbol{x})\varphi^*_\beta(\boldsymbol{x})\varphi^*_\gamma(\boldsymbol{x})\varphi'_\alpha(\boldsymbol{x})\varphi'_\beta(\boldsymbol{x})\varphi'_\gamma(\boldsymbol{x})\prod_{\mu\neq\alpha,\beta,\gamma}\langle\varphi_\mu\mid\varphi'_\mu\rangle,\end{aligned} \tag{25}$$

where σ_α, f_α, and φ_α ($\sigma'_\alpha, f'_\alpha$, and φ'_α) are the spin, flavor, and spatial wave functions for the αth quark in ϕ (ϕ'), respectively.

The KMT matrix elements in baryon systems are obtained as a sum of those for the product wave functions,

$$\begin{aligned}\mathcal{V}_\mathcal{A} &\equiv \langle\psi_\mathcal{A}|V_{\rm KMT}|\psi'_\mathcal{A}\rangle = \langle\psi|V_{\rm KMT}|\mathcal{A}[\psi']\rangle = \sum_{I,J}c^*_I c_J\langle\phi_I|V_{\rm KMT}|\mathcal{A}[\phi'_J]\rangle\\ &= -2g_{\rm D}\sum_{I,J}c^*_I c'_J\sum_P C_P(\phi_I,\phi_J)\,\langle\sigma_I\mid P\sigma'_J\rangle\sum_{\{\alpha,\beta,\gamma\}}F^{\rm KMT}_{\alpha\beta\gamma}(f_I,Pf'_J)R^{\rm KMT}_{\alpha\beta\gamma}(\varphi_I,P\varphi'_J),\end{aligned} \tag{26}$$

where c_I, f_I, and φ_I (c'_J, f'_J, and φ'_J) are the flavor–spin coefficients, flavor configurations, and spatial wave functions of the Ith (Jth) component of the baryon wave function in the bra (ket) state, respectively, and C_P is the color factor.

In Table 3, we show the norm and the diagonal matrix elements of the KMT operator,

$$\hat{T}^{\rm KMT} = \sum_{\{\alpha,\beta,\gamma\}} \varepsilon_{ijk}\, \hat{T}^{u,i}_{\alpha}\, \hat{T}^{d,j}_{\beta}\, \hat{T}^{s,k}_{\gamma}, \tag{27}$$

$$\begin{aligned}\mathcal{T}_{\mathcal{A}} &\equiv \langle \psi_{\mathcal{A}} \mid \hat{T}^{\rm KMT} \mid \psi_{\mathcal{A}} \rangle \\ &= \sum_{I,J} c^*_I c'_J \sum_P C_P(\phi_I, \phi_J)\, \langle \sigma_I \mid P\sigma'_J \rangle \sum_{\{\alpha,\beta,\gamma\}} F^{\rm KMT}_{\alpha\beta\gamma}(f_I, Pf'_J),\end{aligned} \tag{28}$$

in baryons sitting at $\boldsymbol{x} = 0$. Spatial wave functions are assumed to be the same for all quarks, then the norm becomes zero when the 2 baryons have the same flavor and spin. For 1-baryon states, the diagonal matrix elements of the KMT operator are found to be zero.

We have summed up the contributions of all the quark permutations, $3! = 6$, $6! = 720$, and $9! = 362\,880$ for 1-, 2-, and 3-baryons, respectively. We note that $F^{\rm KMT}_{\alpha\beta\gamma}$ is an integer, C_P is a multiple of $1/9$, and $c^*_I c'_J$ is a multiple of $(1/12)^{n-n_\Lambda} \times (1/2)^{n_\Lambda}$ for the diagonal matrix elements in n-baryon systems with n_Λ being the number of Λ. Thus $\mathcal{N}_{\mathcal{A}}$ and $\mathcal{T}_{\mathcal{A}}$ are rational numbers. The genuine 2- and 3-baryon parts of the matrix elements are evaluated by subtracting the contribution in subsystems. For example, for $n_\uparrow n_\downarrow \Lambda_\uparrow$ 3-baryon systems, we subtract the $N\Lambda$ contributions,

$$\mathcal{T}_{3B}(n_\uparrow n_\downarrow \Lambda_\uparrow) = \mathcal{T}(n_\uparrow n_\downarrow \Lambda_\uparrow) - \mathcal{T}(n_\uparrow \Lambda_\uparrow) - \mathcal{T}(n_\downarrow \Lambda_\uparrow) = 4, \tag{29}$$

where $\mathcal{T} = \mathcal{T}_{\mathcal{A}}/\mathcal{N}_{\mathcal{A}}$.

We find that the expectation values of the KMT operator take positive values of 3–20 for $2B$ and $3B$ systems including hyperons. Thus the KMT interaction is confirmed to generate a $3B$ repulsive potential when we have hyperons in $3B$ systems.

The expectation values of the KMT operator $\mathcal{T}_{2B}$ and $\mathcal{T}_{3B}$ are found to be spin dependent: It is larger for larger spin states, e.g., $\mathcal{T}_{2B}((N\Lambda)_{S=1}) > \mathcal{T}_{2B}((N\Lambda)_{S=0})$ and $\mathcal{T}_{3B}((NN\Lambda)_{S=3/2}) > \mathcal{T}_{3B}((NN\Lambda)_{S=1/2})$. Since the KMT operator does not change the quark spin in the nonrelativistic treatment, more quark pairs have the same spin in the bra and ket and a larger matrix element $\mathcal{T}_{\mathcal{A}}$ will appear in larger spin states. We note that the matrix element in the spin quartet state, $\mathcal{T}_{3B}((pn\Lambda)_{S=3/2})$, is much larger than others.

The norms, expectation values of the KMT operator, and its $2B$ and $3B$ parts in all 1-, 2-, 3-octet-baryon states are shown in Appendix.

3.2. *Baryon potentials from the KMT interaction*

We evaluate the $3B$ potential from the KMT interaction (KMT-$3B$ potential) as the expectation value of the $3B$ part of the KMT interaction operator (21) in 3 baryons located at $\mathbf{R}_1$, $\mathbf{R}_2$, and $\mathbf{R}_3$,[1]

$$V^{\rm KMT}_{3B}(\mathbf{R}_1, \mathbf{R}_2, \mathbf{R}_3) = \left. \frac{\mathcal{V}_{\mathcal{A}}(\mathbf{R}_1, \mathbf{R}_2, \mathbf{R}_3)}{\mathcal{N}_{\mathcal{A}}(\mathbf{R}_1, \mathbf{R}_2, \mathbf{R}_3)} \right|_{3B}, \tag{30}$$

[1] Strictly speaking, this is the expectation value of the potential and not the potential itself. As long as the extension of the baryon wave function is large enough compared with the intrinsic extension of the quark wave function, however, the present treatment gives a good estimate of the potential.

where $\mathcal{V}_\mathcal{A}/\mathcal{N}_\mathcal{A}|_{3B}$ denotes the $3B$ potential part of the expectation value. The spatial part of the intrinsic baryon wave function is assumed to be $(0s)^3$; all quarks are assumed to be in the s-wave state of the harmonic oscillator potential and to have the same spatial extension,

$$\varphi_{\boldsymbol{R}}(\boldsymbol{x}) = \left(\frac{2\nu}{\pi}\right)^{3/4} \exp\left(-\nu(\boldsymbol{x}-\boldsymbol{R})^2\right), \tag{31}$$

where $\boldsymbol{R}$ is the position of the baryon and the size parameter ν is related to the size of the quark wave functions b as $\nu = 1/(2b^2)$. The strength of the KMT matrix element for 3 baryons located at the same position ($\mathbf{R}_{1,2,3} = 0$) reads

$$V_{3B}^{\rm KMT}(\mathbf{R}_{1,2,3}=0) = -2g_{\rm D}\mathcal{T}_{3B}\int d^3x\,\varphi_0(\boldsymbol{x})^6 = \frac{-2g_{\rm D}}{(\sqrt{3}\pi b^2)^3}\,\mathcal{T}_{3B} = V_0\,\mathcal{T}_{3B}. \tag{32}$$

By using the parameters $g_{\rm D}\Lambda^5 = -9.29$ and $\Lambda = 631.4$ MeV [32], $b = 0.6$ fm [43] or $b = 0.5562$ fm [44], we find

$$V_0 \equiv \frac{-2g_{\rm D}}{(\sqrt{3}\pi b^2)^3} = \frac{-2g_{\rm D}\Lambda^5}{(\sqrt{3}\pi b^2\Lambda^2)^3}\,\Lambda = \begin{cases} 1.45\,\text{MeV} & (b = 0.6\,\text{fm}), \\ 2.29\,\text{MeV} & (b = 0.5562\,\text{fm}). \end{cases} \tag{33}$$

If we take $g_{\rm D}\Lambda^5 = -12.36$ and $\Lambda = 602.3$ MeV [33], V_0 becomes about 1.68 times larger than the values (33) because V_0 is linearly proportional to $g_{\rm D}$. At finite $\mathbf{R}_{1,2,3}$, the spatial matrix element of the KMT operator is given as

$$\begin{aligned} R^{\rm KMT} &\simeq \int d^3x\,\varphi^*_{\boldsymbol{R}_a}(\boldsymbol{x})\varphi^*_{\boldsymbol{R}_b}(\boldsymbol{x})\varphi^*_{\boldsymbol{R}_c}(\boldsymbol{x})\varphi_{\boldsymbol{R}_d}(\boldsymbol{x})\varphi_{\boldsymbol{R}_e}(\boldsymbol{x})\varphi_{\boldsymbol{R}_f}(\boldsymbol{x}) \\ &= \frac{1}{(\sqrt{3}\pi b^2)^3}\exp\left[-\frac{\nu}{6}\sum_{i<j,i,j=a\sim f}\boldsymbol{R}_{ij}^2\right], \end{aligned} \tag{34}$$

where $\boldsymbol{R}_{ij} = \boldsymbol{R}_i - \boldsymbol{R}_j$ and $\boldsymbol{R}_i$ ($i = a \sim f$) is one of $\boldsymbol{R}_1, \boldsymbol{R}_2$, and $\boldsymbol{R}_3$. When the antisymmetrization effects on the spatial wave function are ignored, other spatial matrix elements ($\prod\langle\varphi_\mu \mid \varphi'_\mu\rangle$ in Eq. (25)) cancel with those from the norm.[2] This prescription provides correct results when the baryons are separated enough or 3 baryons are located at the same spatial point. The KMT-$3B$ potential is then given as

$$V_{3B}^{\rm KMT}(\boldsymbol{R}_1,\boldsymbol{R}_2,\boldsymbol{R}_3) \simeq V_0\mathcal{T}_{3B}\,\exp\left[-\frac{2\nu}{3}(\boldsymbol{R}_{12}^2+\boldsymbol{R}_{23}^2+\boldsymbol{R}_{31}^2)\right]. \tag{35}$$

In Fig. 4, we show the KMT-$3B$ potential $V_{3B}^{\rm KMT}$ for the $NN\Lambda$ system in the $(nn)_{S=0}\Lambda$ and $(np\Lambda)_{S=3/2}$ channels with a linear configuration in which 3 baryons are located at $\mathbf{R}_1 = (-r,0,0)$, $\mathbf{R}_2 = (0,0,0)$, and $\mathbf{R}_3 = (r,0,0)$. We adopt V_0 values evaluated in Eq. (33). The KMT-$NN\Lambda$ potential at $r = 0$ has height 5.8 (9.2) MeV in the $(nn)_{S=0}\Lambda$ channel and 24.2 (38.2) MeV in the

[2] For a more serious discussion, we need to evaluate the spatial factor $R^{\rm KMT}_{\alpha\beta\gamma}$ in Eq. (25) including the overlaps of other quarks, as well as those in the norm. In addition, the KMT matrix element can be finite also in those configurations having $\mathcal{T} = 0$ at zero distance. For example, the $n_\uparrow n_\uparrow \Lambda_\uparrow$ configuration has a zero norm and a zero KMT matrix element due to the Pauli blocking when 3 baryons are located at the same point, but will have a finite norm and a finite KMT matrix element at finite distances. These are beyond the scope of this paper, and we concentrate on the potentials in $NN\Lambda$ and $N\Lambda\Lambda$ channels having finite KMT matrix elements at zero distance.

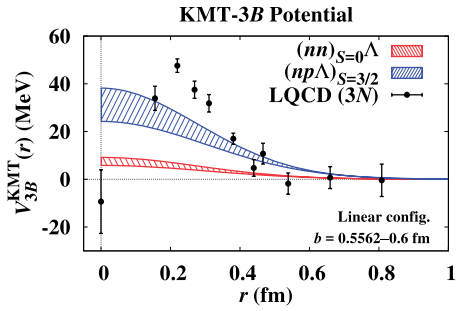

Fig. 4. Three-baryon potential in $(nn)_{S=0}\Lambda$ and $(np\Lambda)_{S=3/2}$ channels generated by the KMT interaction. The shaded area shows the uncertainties from the size parameter. Filled circles show the results of the $3N$ potential obtained in the lattice QCD simulation [23].

$(np\Lambda)_{S=3/2}$ channel for $b = 0.6$ (0.5562) fm, respectively, and the potential range is determined by the baryon size.

We compare the KMT-$NN\Lambda$ potential with the $3N$ potential obtained by using the lattice QCD simulation (LQCD-$3N$ potential) [23]. It is interesting to find that the KMT-$NN\Lambda$ potential and the LQCD-$3N$ potential have the same order of strengths and ranges, while the system is different and they do not need to agree. One of the differences is the short range behavior; the KMT-$NN\Lambda$ potential has a peak at $r = 0$, whereas the LQCD-$3N$ potential is suppressed at $r = 0$.

3.3. KMT-3B potential energy in nuclear matter

We shall now evaluate the KMT-$3B$ potential energy per baryon in nuclear matter. We assume that the density of each baryon is constant; then we get the energy per baryon $W_{3B}^{\rm KMT}$ from the KMT-$3B$ potential as

$$W_{3B}^{\rm KMT} = \frac{1}{\rho_B \Omega}\int d^3R_1\, d^3R_2\, d^3R_3\, \frac{1}{3!}\sum_{B_1,B_2,B_3}\rho(B_1)\,\rho(B_2)\,\rho(B_3)\,V_{3B}^{\rm KMT}(B_1B_2B_3;\boldsymbol{R}_1,\boldsymbol{R}_2,\boldsymbol{R}_3)$$
$$= \frac{W_0}{3!}\left(\frac{\rho_B}{\rho_0}\right)^2\sum_{B_1,B_2,B_3}\frac{\rho(B_1)\rho(B_2)\rho(B_3)}{\rho_B^3}\mathcal{T}_{3B}(B_1B_2B_3), \tag{36}$$

$$W_0 = V_0\left(\sqrt{3}\pi b^2\right)^3\rho_0^2 = -2g_{\rm D}\rho_0^2 \simeq 0.28\,{\rm MeV}, \tag{37}$$

where ρ_B is the baryon density and Ω denotes the spatial volume. It should be noted that W_0 is independent of the baryon size b. The KMT-$3B$ potential energy per baryon in $n\Lambda$ matter is given as

$$W_{n\Lambda}^{\rm KMT}(\rho_B, Y_\Lambda) = W_0\left(\frac{\rho_B}{\rho_0}\right)^2\left[\frac{1}{2}\,Y_n^2\,Y_\Lambda\,\widetilde{\mathcal{T}}_{3B}(NN\Lambda) + \frac{1}{2}\,Y_n\,Y_\Lambda^2\,\widetilde{\mathcal{T}}_{3B}(N\Lambda\Lambda)\right], \tag{38}$$

where Y_n and Y_Λ represent the density fractions of n and Λ respectively, with $Y_n = \rho_n/\rho_B$ and $Y_\Lambda = \rho_\Lambda/\rho_B$, and $\widetilde{\mathcal{T}}_{3B}(NN\Lambda)$ and $\widetilde{\mathcal{T}}_{3B}(N\Lambda\Lambda)$ are the spin-averaged KMT matrix elements

$$\widetilde{\mathcal{T}}_{3B}(NN\Lambda) = \frac{1}{8}\sum_{\sigma_1,\sigma_2,\sigma_3}\mathcal{T}_{3B}(n_{\sigma_1}n_{\sigma_2}\Lambda_{\sigma_3}) = \frac{1}{2}\,\mathcal{T}_{3B}((nn)_{S=0}\Lambda) = 2, \tag{39}$$

$$\widetilde{\mathcal{T}}_{3B}(N\Lambda\Lambda) = \frac{1}{8}\sum_{\sigma_1,\sigma_2,\sigma_3}\mathcal{T}_{3B}(N_{\sigma_1}\Lambda_{\sigma_2}\Lambda_{\sigma_3}) = \frac{1}{2}\,\mathcal{T}_{3B}(N(\Lambda\Lambda)_{S=0}) = \frac{7}{2}, \tag{40}$$

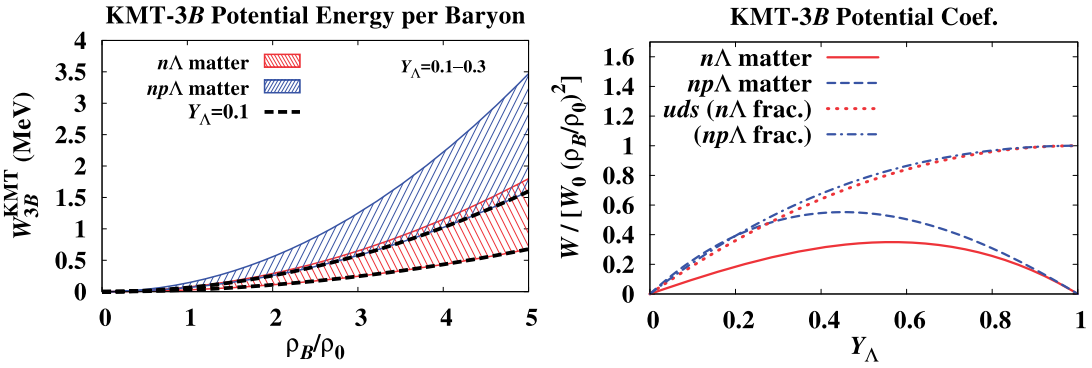

Fig. 5. KMT-3B potential energy per baryon in $n\Lambda$ and $np\Lambda$ matter (left), and the coefficients of the potential energy per baryon, $W^{\rm KMT}/[W_0\,(\rho_B/\rho_0)^2]$ in $n\Lambda$, $np\Lambda$, and quark matter (right).

where the $(S,T)=(0,1)$ pair is taken for $NN\Lambda$. Note that $Y_n+Y_\Lambda=1$ in $n\Lambda$ matter. For $np\Lambda$ matter, we find

$$W^{\rm KMT}_{pn\Lambda}(\rho_B,Y_\Lambda)=W_0\left(\frac{\rho_B}{\rho_0}\right)^2\left[\frac{1}{2}\,(Y_n^2+Y_p^2)\,Y_\Lambda\,\widetilde{\mathcal{T}}_{3B}(NN\Lambda)+\frac{1}{2}\,(Y_n+Y_p)\,Y_\Lambda^2\,\widetilde{\mathcal{T}}_{3B}(N\Lambda\Lambda)\right.$$
$$\left.+Y_n\,Y_p\,Y_\Lambda\,\widetilde{\mathcal{T}}_{3B}(np\Lambda)\right], \tag{41}$$

where $\widetilde{\mathcal{T}}_{3B}(np\Lambda)$ is the spin-averaged KMT matrix element in the $np\Lambda$ system,

$$\widetilde{\mathcal{T}}_{3B}(np\Lambda)=\frac{1}{4}\left[\mathcal{T}_{3B}((np\Lambda)_{S=3/2})+2\mathcal{T}_{3B}(n_\uparrow p_\downarrow\Lambda)+\mathcal{T}_{3B}(n_\uparrow p_\uparrow\Lambda_\downarrow)\right]=\frac{17}{2}. \tag{42}$$

Note that $Y_n+Y_p+Y_\Lambda=1$ in the $np\Lambda$ matter.

In the left panel of Fig. 5, we show the KMT-3B potential energy per baryon in $n\Lambda$ and $np\Lambda$ matter. Each shaded area corresponds to $0.1\le Y_\Lambda\le 0.3$ and neutron and proton fractions are taken to be $Y_n=1-Y_\Lambda$ and $Y_n=Y_p=(1-Y_\Lambda)/2$ for $n\Lambda$ and $np\Lambda$ matter, respectively. The KMT-3B potential energy per baryon amounts to be $W^{\rm KMT}_{3B}=0.027$ and 0.064 MeV at $(\rho_B,Y_\Lambda)=(\rho_0,0.1)$ in $n\Lambda$ and $np\Lambda$ matter, respectively. At a higher density and a larger Λ fraction, the KMT-3B potential is found to reduce the nuclear symmetry energy slightly; $W^{\rm KMT}_{3B}=0.65$ and 1.25 MeV at $(\rho_B,Y_\Lambda)=(3\rho_0,0.3)$ in $n\Lambda$ and $np\Lambda$ matter, respectively, and then the KMT-3B potential reduces the difference between the energy per baryon in neutron matter with Λ admixture ($n\Lambda$ matter) and in symmetric nuclear matter with Λ admixture ($np\Lambda$ matter) by about 0.6 MeV.

It may be instructive to compare the above potential energy with that in quark matter having the same uds quark fractions:

$$W^{\rm KMT}_{uds}(\rho_B)=W_0\left(\frac{\rho_B}{\rho_0}\right)^2 Y_u\,Y_d\,Y_s, \tag{43}$$

$$Y_u=\rho_u/\rho_B=2Y_p+Y_n+Y_\Lambda,\qquad Y_d=Y_p+2Y_n+Y_\Lambda,\qquad Y_s=Y_\Lambda. \tag{44}$$

It should be noted that only the residual interaction contribution is considered here, and other contributions coming from the condensates are not counted. In the right panel of Fig. 5, we compare the coefficients of the potential energy per baryon $W^{\rm KMT}/[W_0\,(\rho_B/\rho_0)^2]$ in $n\Lambda$, $np\Lambda$, and quark matter. For a small strange quark fraction (small Y_Λ), we note that the quark matter estimate agrees with the baryonic matter estimate in $np\Lambda$ matter, while the baryonic matter estimate results in weaker KMT-3B repulsion in $n\Lambda$ matter.

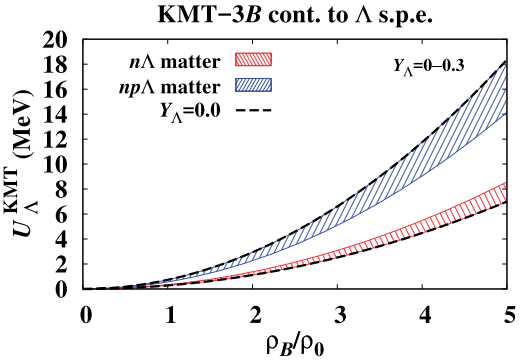

Fig. 6. KMT-3B potential contribution to Λ single particle energy.

Finally, we discuss the KMT-3B potential contribution to the Λ single particle energy,

$$U_\Lambda = \frac{\partial\,(\rho_B W)}{\partial \rho_\Lambda}. \tag{45}$$

In $n\Lambda$ and $pn\Lambda$ matter, we find

$$U^{\rm KMT}_{\Lambda(n\Lambda)}(\rho_B, Y_\Lambda) = W_0 \left(\frac{\rho_B}{\rho_0}\right)^2 \left[\frac{1}{2}\, Y_n^2\, \widetilde{\mathcal{T}}_{3B}(NN\Lambda) + Y_n\, Y_\Lambda\, \widetilde{\mathcal{T}}_{3B}(N\Lambda\Lambda)\right], \tag{46}$$

$$U^{\rm KMT}_{\Lambda(pn\Lambda)}(\rho_B, Y_\Lambda) = W_0 \left(\frac{\rho_B}{\rho_0}\right)^2 \left[\frac{1}{2}\,(Y_n^2 + Y_p^2)\, \widetilde{\mathcal{T}}_{3B}(NN\Lambda) + (Y_n + Y_p)\, Y_\Lambda\, \widetilde{\mathcal{T}}_{3B}(N\Lambda\Lambda) + Y_n\, Y_p\, \widetilde{\mathcal{T}}_{3B}(np\Lambda)\right]. \tag{47}$$

In Fig. 6, we show the Λ single particle potential in $n\Lambda$ and $pn\Lambda$ matter. The neutron and proton fractions in $np\Lambda$ matter are again taken to be $Y_n = Y_p = (1 - Y_\Lambda)/2$. The average $pn\Lambda$ matrix element is larger than that of $nn\Lambda$, since we have more combinations of uds in $pn\Lambda$ matter. As a result, Λ feels more repulsion in symmetric matter than in pure neutron matter. The KMT-3B potential contribution to the Λ single particle energy is found to be $U^{\rm KMT}_{\Lambda(n\Lambda)} \simeq 0.28\,$MeV and $U^{\rm KMT}_{\Lambda(pn\Lambda)} \simeq 0.73\,$MeV at $\rho_B = \rho_0$ in neutron matter and symmetric nuclear matter ($n\Lambda$ and $pn\Lambda$ matter at $Y_\Lambda = 0$), respectively. These contributions are not large, but would be measurable in high-resolution experiments on the Λ separation energy of hyperisotopes such as ${}^{40}_{\Lambda}$K and ${}^{48}_{\Lambda}$K [45].

4. Summary

We have evaluated the expectation value of the determinant interaction of quarks, the Kobayashi–Maskawa [28,29] and 't Hooft [30,31] (KMT) interaction, in 3-baryon systems, and have discussed the 3-baryon potential from the KMT interaction. The KMT vertex gives rise to such a 3-quark interaction that all the u, d and s quarks need to participate. Then the KMT interaction is expected to generate potentials among 3 baryons that include at least 1 hyperon. The KMT interaction is responsible for the $U(1)_A$ anomaly, and its strength is determined from the η' mass [32,33]. The negative sign of the strength parameter in the Lagrangian generates a repulsive 3-quark interaction. Repulsive potential among 3 baryons including hyperons may help to solve the hyperon puzzle of 2-solar-mass neutron stars [1,2].

The expectation value of the KMT operator (Eq. (27)) is obtained for the 2- and 3-baryon ($2B$ and $3B$) states consisting of nucleons and Λ baryons, where baryons are assumed to be located at the same spatial point. We have adopted nonrelativistic $(0s)^3$ wave functions for octet baryons, where a common spatial wave function is assumed for all quarks. The $2B$ and $3B$ states are given as the product of baryon wave functions antisymmetrized under the quark exchanges. The KMT operator is found to take positive expectation values of 3–20 for $2B$ and $3B$ systems consisting of N and at least one Λ particle. Thus the KMT interaction is confirmed to generate $3B$ repulsive potential in $NN\Lambda$ and $N\Lambda\Lambda$ systems. The expectation value of the KMT operator, $\mathcal{T}_{2B}$ and $\mathcal{T}_{3B}$, is found to be larger for the larger spin state, $\mathcal{T}_{2B}((N\Lambda)_{S=1}) > \mathcal{T}_{2B}((N\Lambda)_{S=0})$ and $\mathcal{T}_{3B}((NN\Lambda)_{S=3/2}) > \mathcal{T}_{3B}((NN\Lambda)_{S=1/2})$. Since the KMT operator does not change the quark spin in the nonrelativistic treatment, there can be more quark pairs having the same spin in the bra and ket of larger spin states and the expectation value of the KMT operator tends to be larger. We also note that the matrix element in the spin quartet state, $\mathcal{T}_{3B}((pn\Lambda)_{S=3/2}$, is much larger than others.

We have evaluated the $3B$ potential from the KMT interaction (KMT-$3B$ potential). The strength of the $3B$ potential is calculated by using the harmonic oscillator wave function of quarks adopted in the quark-cluster model analyses of $2B$ potentials [43,44] and the strength of the KMT interaction obtained from the η' mass analyses [32]. The obtained $NN\Lambda$ potential from the KMT interaction has height 5.8–9.2 MeV in the $(nn)_{S=0}\Lambda$ channel and 24.2–38.2 MeV in the $(np\Lambda)_{S=3/2}$ channel at zero distance, and the potential range is determined by the baryon size. The strength and the range of the $3B$ potential in the linear configuration are found to be similar to those from the $3N$ potential obtained in the lattice QCD simulation [23] except for the short range region. Since the determinant interaction strength has uncertainty and can be larger by some factor [36], the 3-baryon repulsion including Λ may be larger than that for 3 nucleons. It is interesting to examine this feature in lattice QCD.

The KMT-$3B$ potential energy per baryon in nuclear matter $W_{3B}^{\rm KMT}$ and the KMT-$3B$ potential contribution to the Λ single particle potential $U_\Lambda^{\rm KMT}$ are also estimated. The KMT-$3B$ contribution to the equation of state, $W_{3B}^{\rm KMT}$, is found to be small; $W_{3B}^{\rm KMT} \simeq 0.05$ MeV and 0.1 MeV for $n\Lambda$ and $np\Lambda$ matter at $(\rho_B, Y_\Lambda) = (\rho_0, 0.1)$, respectively. The KMT-$3B$ contribution to the Λ single particle potential $U_\Lambda^{\rm KMT}$ is not large but would be visible; $U_\Lambda^{\rm KMT} \simeq 0.56$ MeV and 1.2 MeV in $n\Lambda$ and $np\Lambda$ matter at $\rho_B = \rho_0$, respectively. The difference is small, but may be detectable in a high-precision experiment on the separation energies of hyperisotopes such as ${}^{40}_{\Lambda}$K and ${}^{48}_{\Lambda}$K [45]. At $\rho_B = 3\rho_0$, $U_\Lambda^{\rm KMT}$ amounts to 2.5 MeV and 6.6 MeV in $n\Lambda$ and $np\Lambda$ matter, respectively.

In the present study, we have considered only the contribution of the 3-quark potential from the determinant interaction. It is desired to take account of the 2-quark potential and 1-quark mass shift simultaneously in order to fully account for the effects of the determinant interaction, where we need to care for the flavor SU(3) symmetry breaking via the quark condensates $\langle\bar{u}u\rangle$, $\langle\bar{d}d\rangle$, and $\langle\bar{s}s\rangle$. It may be also necessary to include the difference and modification of the nucleon and hyperon size in vacuum and medium. Another major simplification made in this work is the nonrelativistic limit treatment of the interaction. At high baryon densities such as 3–$5\rho_0$, relativistic effects, including the lower component of the quark wave function [40], need to be included. In order to solve the hyperon puzzle of massive neutron stars, we need to find the mechanism to generate additional Λ single particle potential $\Delta U_\Lambda \sim 100$ MeV at around $\rho_B = 3\rho_0$, and the KMT-$3B$ potential explains 2%–7% of the required repulsion. Other 3-quark interactions such as the confinement potential [46] can also contribute to the $3B$ potential.

Acknowledgements

This work was supported in part by the Grants-in-Aid for Scientific Research on Innovative Areas from MEXT (Nos. 24105008 and 24105001), Grants-in-Aid for Scientific Research from JSPS (Nos. 15K05079, 15H03663, 16K05349, 16K05350). K.M. was supported in part by the National Science Center, Poland under Maestro Grant No. DEC-2013/10/A/ST2/00106. K.K. was supported in part by Grant-in-Aid No. 26-1717 from JSPS.

Appendix. Expectation values of the KMT operator in 1-, 2-, and 3-baryon systems

We showed in Sect. 3 the expectation values of the KMT operator in some selected channels including N and Λ. In Fig. 7, we show the results for all states consisting of 1, 2 and 3 octet baryons

$$|\psi_{\mathcal{A}}\rangle = |B_\sigma\rangle, \qquad \frac{\mathcal{A}}{\sqrt{6!}}|B_\sigma B'_{\sigma'}\rangle, \qquad \frac{\mathcal{A}}{\sqrt{9!}}|B_\sigma B'_{\sigma'} B''_{\sigma''}\rangle. \tag{A.1}$$

Channels are sorted according to strangeness quantum number.

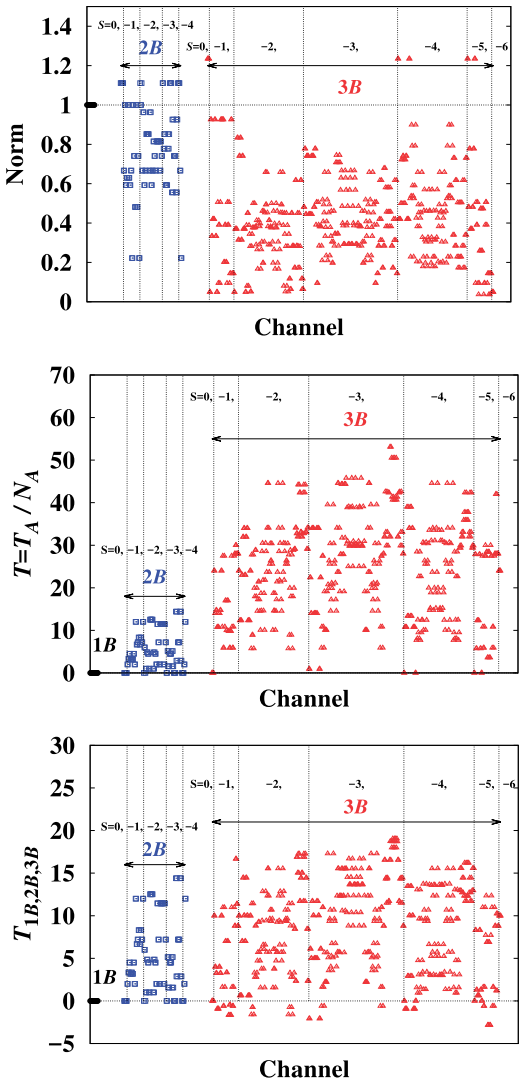

Fig. 7. Norm (top), expectation value of the KMT operator (middle) and its nB part (bottom) in 1-, 2-, and 3-octet-baryon states.

As already discussed in Refs. [42,47], the norm takes small values in, e.g., $(N\Sigma)_{(S,T)=(1,3/2)}$, $(\Xi^-\Xi^0)_{S=1}$ ($\mathcal{N}_\mathcal{A} = 2/9$) and $(N\Sigma^0)_{S=1}$, ($\mathcal{N}_\mathcal{A} = 13/27$) in $2B$ states[3] and $\Lambda(\Xi^-\Xi^0)_{S=1}$ ($\mathcal{N}_\mathcal{A} = 1/27$), $(nn)_{S=0}\Sigma^-$, $n(\Sigma^-\Sigma^-)_{S=0}$, $(pp)_{S=0}\Sigma^+$, $p(\Sigma^+\Sigma^+)_{S=0}$, $(\Xi^-\Xi^-)_{S=0}\Xi^0$, $\Xi^-(\Xi^0\Xi^0)_{S=0}$, ($\mathcal{N}_\mathcal{A} = 4/81$) in $3B$ states, where repulsion from the quark-Pauli effects is expected.

The expectation value of the KMT operator takes large values in, e.g., $(\Lambda\Xi)_{S=1}$ ($\mathcal{T} = 72/5$), $p_\uparrow\Xi^-_\downarrow$, $p_\downarrow\Xi^-_\uparrow$, $n_\uparrow\Xi^0_\downarrow$, $n_\downarrow\Xi^0_\uparrow$, $\Sigma^-_\uparrow\Sigma^+_\downarrow$, $\Sigma^-_\downarrow\Sigma^+_\uparrow$ ($\mathcal{T} = 288/23$), $(n\Sigma^-)_{S=1}$, $(p\Sigma^+)_{S=1}$, $(\Xi^-\Xi^0)_{S=1}$, ($\mathcal{T} = 12$) in $2B$ states and $(\Sigma\Sigma\Sigma)_{S=3/2}$ ($\mathcal{T} = 584/11$), $(p\Lambda\Xi^-)_{S=3/2}$ $(n\Lambda\Xi^0)_{S=3/2}$ ($\mathcal{T} = 2374/47$), $p_\downarrow\Lambda_\uparrow\Xi^-_\uparrow$ $p_\uparrow\Lambda_\downarrow\Xi^-_\downarrow$ $n_\downarrow\Lambda_\uparrow\Xi^0_\uparrow$ $n_\uparrow\Lambda_\downarrow\Xi^0_\downarrow$ ($\mathcal{T} = 2106/46$) in $3B$ states. In some of $NN\Sigma$, $N\Lambda\Sigma$, $N\Sigma\Xi$, $N\Xi\Xi$, $\Lambda\Sigma\Sigma$, $\Sigma\Xi\Xi$, and $\Sigma\Sigma\Xi$ states, the $3B$ part of the expectation value is found to be negative, while $\mathcal{T}$ is positive.

References

[1] P.B. Demorest, T. Pennucci, S.M. Ransom, M.S.E. Roberts, and J.W.T. Hessels, Nature **467**, 1081 (2010) [arXiv:1010.5788 [astro-ph.HE]] [Search INSPIRE].
[2] J. Antoniadis et al., Science **340**, 6131 (2013) [arXiv:1304.6875 [astro-ph.HE]] [Search INSPIRE].
[3] N.K. Glendenning and S.A. Moszkowski, Phys. Rev. Lett. **67**, 2414 (1991).
[4] S. Nishizaki, Y. Yamamoto, and T. Takatsuka, Prog. Theor. Phys., **108**, 703 (2002).
[5] Z.H. Li and H.J. Schulze, Phys. Rev. C **78**, 028801 (2008).
[6] C. Ishizuka, A. Ohnishi, K. Tsubakihara, K. Sumiyoshi, and S. Yamada, J. Phys. G **35**, 085201 (2008) [arXiv:0802.2318 [nucl-th]] [Search INSPIRE].
[7] K. Tsubakihara, H. Maekawa, H. Matsumiya, and A. Ohnishi, Phys. Rev. C **81**, 065206 (2010) [arXiv:0909.5058 [nucl-th]] [Search INSPIRE].
[8] K. Masuda, T. Hatsuda, and T. Takatsuka, Astrophys. J. **764**, 12 (2013) [arXiv:1205.3621 [nucl-th]] [Search INSPIRE].
[9] K. Masuda, T. Hatsuda, and T. Takatsuka, Prog. Theor. Exp. Phys. **2013**, 073D01 (2013) [arXiv:1212.6803 [nucl-th]] [Search INSPIRE].
[10] L. Adamczyk et al., Phys. Rev. Lett. **112**, 162301 (2014) [arXiv:1401.3043 [nucl-ex]] [Search INSPIRE].
[11] Y. Nara, H. Niemi, A. Ohnishi, and H. Stoecker, Phys. Rev. C **94**, 034906 (2016) [arXiv:1601.07692 [hep-ph]] [Search INSPIRE].
[12] S. Weissenborn, D. Chatterjee, and J. Schaffner-Bielich, Phys. Rev. C **85**, 065802 (2012); **90**, 019904 (2014) [erratum] [arXiv:1112.0234 [astro-ph.HE]] [Search INSPIRE].
[13] W. Freeman and D. Toussaint, Phys. Rev. D **88**, 054503 (2013) [arXiv:1204.3866 [hep-lat]] [Search INSPIRE].
[14] J. Fujita and H. Miyazawa, Prog. Theor. Phys. **17**, 360 (1957).
[15] S.C. Pieper and R.B. Wiringa, Ann. Rev. Nucl. Part. Sci. **51**, 53 (2001) [arXiv:nucl-th/0103005] [Search INSPIRE].
[16] Y. Yamamoto, T. Furumoto, N. Yasutake, and T.A. Rijken, Phys. Rev. C **90**, 045805 (2014) [arXiv:1406.4332 [nucl-th]] [Search INSPIRE].
[17] E. Epelbaum, H.-W. Hammer, and U.-G. Meissner, Rev. Mod. Phys. **81**, 1773 (2009) [arXiv:0811.1338 [nucl-th]] [Search INSPIRE].
[18] R. Machleidt and D.R. Entem, Phys. Rept. **503**, 1 (2011) [arXiv:1105.2919 [nucl-th]] [Search INSPIRE].
[19] B. Friedman and V.R. Pandharipande, Nucl. Phys. A **361**, 502 (1981).
[20] A. Akmal, V.R. Pandharipande, and D.G. Ravenhall, Phys. Rev. C **58**, 1804 (1998) [arXiv:nucl-th/9804027] [Search INSPIRE].
[21] M. Kohno, Phys. Rev. C **88**, 064005 (2013) [arXiv:1309.4556 [nucl-th]] [Search INSPIRE].
[22] K. Sekiguchi, et al., Phys. Rev. C. **65**, 034003 (2002).

[3] To describe the $(N\Sigma)_{(S,T)=(0,1/2)}$ state having $\mathcal{N}_\mathcal{A} = 1/9$ or the $(N\Lambda - N\Sigma)_{(S,T)=(0,1/2)}$ coupled state having $\mathcal{N}_\mathcal{A} = 0, 10/9$, off-diagonal matrix elements have to be accounted for.

[23] T. Doi, S. Aoki, T. Hatsuda, Y. Ikeda, T. Inoue, N. Ishii, K. Murano, H. Nemura, and K. Sasaki, Prog. Theor. Phys. **127**, 723 (2012) [arXiv:1106.2276 [hep-lat]] [Search INSPIRE].
[24] D. Lonardoni, F. Pederiva, and S. Gandolfi, Phys. Rev. C **89**, 014314 (2014) [arXiv:1312.3844 [nucl-th]] [Search INSPIRE].
[25] A.R. Bodmer, Q.N. Usmani, and J. Carlson, Phys. Rev. C **29**, 684(R) (1984).
[26] D. Lonardoni, A. Lovato, S. Gandolfi, and F. Pederiva, Phys. Rev. Lett. **114**, 092301 (2015) [arXiv:1407.4448 [nucl-th]] [Search INSPIRE].
[27] T. Miyatsu, S. Yamamuro, and K. Nakazato, Astrophys. J. **777**, 4 (2013) [arXiv:1308.6121 [astro-ph.HE]] [Search INSPIRE].
[28] M. Kobayashi and T. Maskawa, Prog. Theor. Phys. **44**, 1422 (1970).
[29] M. Kobayashi, H. Kondo, and T. Maskawa, Prog. Theor. Phys. **45**, 1955 (1971).
[30] G. 't Hooft, Phys. Rev. D **14**, 3432 (1976); **18**, 2199 (1978) [erratum].
[31] G. 't Hooft, Phys. Rept. **142**, 357 (1986).
[32] T. Hatsuda and T. Kunihiro, Phys. Rept. **247**, 221 (1994) [arXiv:hep-ph/9401310] [Search INSPIRE].
[33] P. Rehberg, S.P. Klevansky, and J. Hufner, Phys. Rev. C **53**, 410 (1996) [arXiv:hep-ph/9506436] [Search INSPIRE].
[34] Y. Nambu and G. Jona-Lasinio, Phys. Rev. **122**, 345 (1961).
[35] Y. Nambu and G. Jona-Lasinio, Phys. Rev. **124**, 246 (1961).
[36] M. Takizawa, Y. Nemoto and M. Oka, Phys. Rev. D **55**, 4083 (1997).
[37] T. Schäfer and E.V. Shuryak, Rev. Mod. Phys. **70**, 323 (1998).
[38] S. Takeuchi and M. Oka, Phys. Rev. Lett. **66**, 1271 (1991).
[39] R.L. Jaffe, Phys. Rev. Lett. **38**, 195 (1977); **38**, 617 (1977) [erratum].
[40] O. Morimatsu and M. Takizawa, Nucl. Phys. A **554**, 635 (1993).
[41] H. Toki, Y. Suzuki, and K.T. Hecht, Phys. Rev. C **26**, 736 (1982).
[42] C. Nakamoto and Y. Suzuki, Phys. Rev. C **94**, 035803 (2016) [arXiv:1606.07225 [nucl-th]] [Search INSPIRE].
[43] M. Oka and K. Yazaki, Prog. Theor. Phys. **66**, 572 (1981).
[44] Y. Fujiwara, Y. Suzuki, and C. Nakamoto, Prog. Part. Nucl. Phys. **58**, 439 (2007) [arXiv:nucl-th/0607013] [Search INSPIRE].
[45] F. Garibaldi et al. [JLab Hypernuclear Collaboration] JLab C12-15-008 (2016).
[46] T.T. Takahashi, H. Suganuma, Y. Nemoto, and H. Matsufuru, Phys. Rev. D **65**, 114509 (2002) [arXiv:hep-lat/0204011] [Search INSPIRE].
[47] M. Oka, K. Shimizu, and K. Yazaki, Nucl. Phys. A **464**, 700 (1987).